

STUDY OF THE LIGHT CURVE OF LSI+61°303

Josep-Maria Paredes

Departament de Física de la Terra i del Cosmos
Universitat de Barcelona. España

RESUMEN. Se presenta un modelo para explicar la variación óptica observada en LSI+61°303 basado en las deformaciones de la estrella primaria producidas por un objeto compacto en un sistema excéntrico.

ABSTRACT. A model based on deformations of the primary star by a compact star in an eccentric system is presented for explaining the optical variability observed in LSI+61°303.

Key words: STARS-VARIABLE -- X-RAY-BINARY

I. INTRODUCTION

The radiostar LSI+61°303 is the only star of the Northern hemisphere (except pulsars) which presents radio periodicity (Taylor and Gregory 1982, 1984; Coe et al. 1983), with a period of 26.496 days. It is a weak (10^{33} erg s⁻¹) X-ray source (Bignami et al. 1981) and it has been suggested as the optical counter part of the γ -ray source CG135+01 (Perotti et al. 1980; Pollock et al. 1981). The values obtained from radial velocity observations are consistent with the radio period and give support to the presence of a companion star (Hutchings and Crampton 1981). UBVRI photometric observations show an optical variability which roughly correlates with the radio light curve (Paredes and Figueras 1986). A model based on deformations of the primary star by a compact star in an eccentric system is carried out for explaining the optical variability observed in LSI+61°303.

II. PHOTOMETRIC OBSERVATIONS

The UBV photometric observations of LSI+61°303, published by Bartolini et al. (1983), point out that this star does not exhibit light variations correlated with the radio light period. Because of the very poor phase coverage of those photometric observations we made new UBVRI observations of this star for ten days, during its maximum radio luminosity. The observations were performed at Calar Alto with the 1.23 m telescope of the Centro Astronómico Hispano-Alemán (C.A.H.A.). The telescope was equipped with a one channel photometer in conjunction with a dry-ice cooled RCA31034 photomultiplier and the conventional UBVRI Johnson system filters. The reduction of the differential photometry measurements was done by averaging, per night, the four magnitude increments obtained between the star and the comparison star, previous temporary interpolation of the last one. The photometric results in V magnitude are plotted in Figure 1. These data indicate that the star exhibits a clearly defined light variation. During the part of the orbital period covered by our observations, the optical light seems to follow the radio light curve given by Taylor and Gregory (1984).

III. DEFORMATIONS OF THE PRIMARY STAR

The accretion model, proposed by Taylor and Gregory (1982, 1984) for explaining the periodicity of the radio emission, is based on multiple shock fronts produced as a result of supercritical Roche lobe overflow at periastron of a highly eccentric orbit. In this context, we expect gravitational deformations of the primary by the secondary star, the deformations being greater near periastron. As a consequence it will appear a redistribution of the surface temperature, that will produce magnitude variations. These variations, which would be stronger near periastron, could explain the observed optical variability.

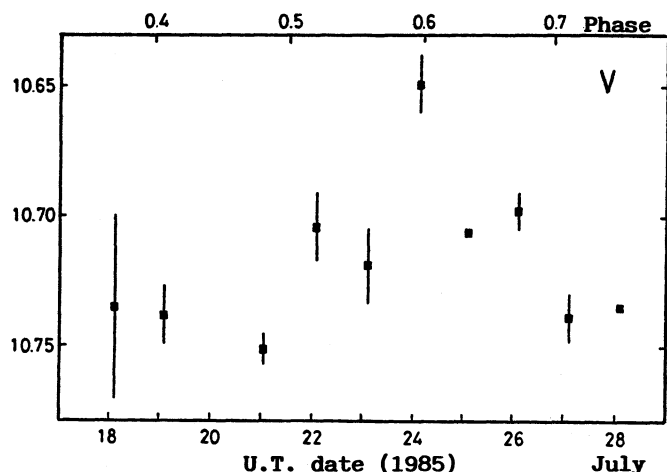


Fig 1. V magnitudes of LSI+61°303 versus U.T.Date and radio phase calculated adopting phase zero at Julian Date 2443366.775 and a period of 26.496 days. The error bars denote the rms of the mean.

In order to carry out a quantitative study of light variations produced by deformations we have employed the program WINK, created by Wood (1971,1973). For a given set of elements that define a model of binary system, the program generates light curves by numerical integration over the apparent disks of the stars. The surface intensities of the stars are given by the effective temperatures and the Planck radiation law in combination with the usual laws for linear limb darkening and gravity brightening.

Wood's model assumes that the stars can be represented by triaxial ellipsoids and allows for eccentric orbits. It takes also into account gravitational and rotational distortions. It is restricted to the case of synchronous rotation of the stars and assumes a constant deformation of the components along the orbit.

However we are interested in working with variable deformations along the orbit and with different rotational velocities. The introduction of these new options in the program WINK and the possibility of working with stellar atmosphere models instead of the standard Planck model was performed by Clausen et al. (1977). We have used this, including also the stellar atmosphere model given by Kurucz (1979).

Since we consider our system being formed by a class III or V young star (Paredes and Figueras 1986; Hutchings and Crampton 1981) and a compact star, the luminous contribution of the compact star in the light curve is not significant, so the physical parameters assigned to the compact star have no repercussion in the generated light curve. The parameters that remain invariable during the calculation process are

limb darkening coefficient, $u = 0.34$	gravity brightening, $\beta = 0.25$
equatorial temperature, $T = 30000 \text{ K}$	time of conjunction, $t = 0$
reflection albedo, $w = 1$	period (days), $P = 26.496$
quadrature magnitude, $quad = 10.74$	log surface gravity, $g = 4$
wavelength, $\lambda = 5500 \text{ \AA}$	

The value of u has been obtained from Carbon and Gingerich (1969).

IV. PARAMETERS OF THE BINARY SYSTEM

The parameters we have varied in order to find which combination of them give us light curves similar to the observed are :

rnot : orbital semi-major axis length. According to third Kepler's law and with a fixed value of the period, the value of the semi-major axis will be determined only for the total mass of the system. The values given to the mass of the primary star (pm) and to the mass of the secondary star (sm) are

$$\begin{aligned} sm &= 1 - 1.5 - 2 M_{\odot} \\ pm &= 1 - 2 - 3 - \dots - 15 M_{\odot} \end{aligned}$$

A : unperturbed spherical radius of the primary star. Its values have been 10 - 11 - 12.. .. - 20 R_{\odot} and 25 - 30 - 35 R_{\odot} .

e : orbital eccentricity. For values of the eccentricity smaller than 0.4, and typical values of mass and radius, the light curves did not show any light variation. Values near 0.4 showed a slight light variation, weaker than the observed. For values of the eccentricity greater than 0.75 the light curve generated was sharp and narrow as a consequence of the great deformation of the primary and the high velocity of the secondary star in the periastron. The systematic calculation of light curves has been performed for values $0.45 \leq e \leq 0.75$, at intervals of 0.05

Ω/Ω_K : angular velocity of rotation referred to the synchronous value. We have taken into account two cases

a) $\Omega/\Omega_K = 1$. The angular velocity of rotation of the primary star is equal to the average orbital angular velocity (synchronous rotation);

b) case in which the rotational velocity of the primary star equals the periastron orbital angular velocity. The relation between angular velocity at periastron (referred to the average orbital angular velocity) and eccentricity is given by

$$\Omega_{\text{periastron}} / \Omega_K = \left(\frac{1+e}{1-e} \right)^{3/2}$$

ω : longitude of periastron. The influence of this parameter on the light curve is reflected in Figure 2. For a fixed value of inclination (90° in this case), and for a given value of ω , we have assigned the phase of the maximum of the observed light curve (0.6) to the maximum of the generated light curve. As we can observe in Figure 2, the only symmetric curve corresponds to the case $\omega = 180^\circ$. It is an expected result considering the geometry and the redistribution of temperatures, according to Von Zeipel law, produced as a consequence of deformations in the primary star induced by the secondary at periastron (indicated with P in the figure). The systematic study was first carried out with values of the longitude of periastron of 0, 60, 120, 180, 240 and 300 degrees. The generated light curves more similar to the observed were obtained with the value $\omega = 180^\circ$, so we adopted this value in a second phase. A behavior similar to the one shown in Figure 2 was obtained with an inclination of 45° .

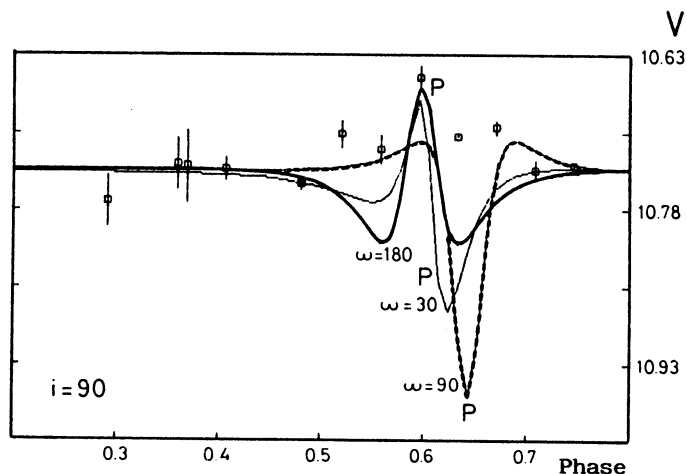


Fig. 2 Generated light curves for different values of longitude of periastron and for a fixed value of inclination. The squares are the observed points. P means periastron.

i : inclination. Figure 3 shows the variations of the generated light curves for different values of inclination and for a fixed value of longitude of periastron ($\omega = 180^\circ$). The behavior of these curves is not surprising. The primary star is being deformed by the secondary before the periastron pass, and for inclination 90° we can see the deformed part of the star pointing us, producing the minimum. When the secondary star is at periastron, we cannot see directly the most deformed part of the star but the zones with radius smaller than

before the deformation. These zones produce the maximum. When the inclination is 0°, the minima disappear because we never see directly the zones of greater radius, id est, the colder. In the systematic study we have worked first with inclination values of 0, 30, 60 and 90 degrees. The greatest values of inclination gave us light curves very different from the observed, so we centered our attention on values 0 and 30 degrees.

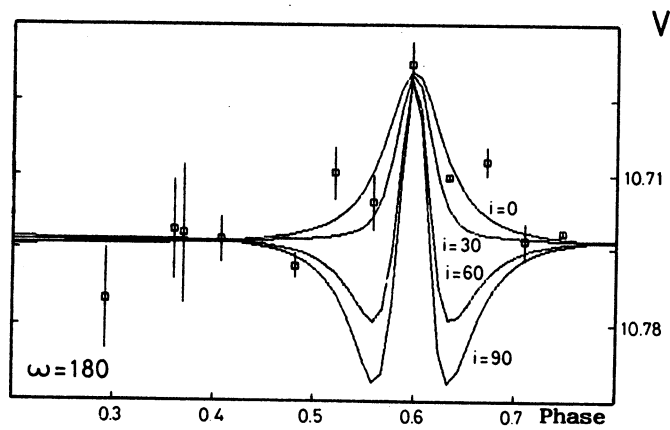


Fig. 3 Generated light curves for different values of inclination and a fixed value for periastron longitude.

V. STATISTICAL PARAMETER

In order to treat the great quantity of light curves generated by the different values given to the variable parameters, we have defined a statistical parameter omc given by

$$omc = \left(\frac{\sum_{i=1}^{nobs} \left(\frac{om(i) - cm(i)}{\sigma(i)} \right)^2}{nobs} \right)^{1/2}$$

where

om(i) : ith observed magnitude , sigma(i) : ith error of the observed magnitude
cm(i) : ith calculated magnitude , nobs : number of observed points.

The observed magnitudes, shown in Table 1, have been obtained by Paredes and Figueras (1986) and by Torra and Nuñez (1986).

TABLE 1. Values of observed magnitudes

Phase	0.29	0.36	0.37	0.41	0.48	0.52	0.56	0.60	0.63	0.67	0.71	0.75
V	10.769	10.734	10.736	10.739	10.752	10.705	10.720	10.650	10.707	10.699	10.740	10.736
sigma	0.026	0.026	0.035	0.011	0.006	0.013	0.014	0.011	0.004	0.007	0.009	0.004

The omc values verifying $1 \leq omc \leq 2$, indicate a similarity between the generated curves and the observed points. If we generate a flat curve, the value obtained of omc is 3.9 For example, the values of omc corresponding to the light curves of Figure 3 are

i	0°	30°	60°	90°
omc	1.69	2.23	6.02	8.41

It is interesting to observe the behavior of omc as a function of the mass of primary star shown in Figure 4, for different values of inclination. The points in the figure have been calculated for the case $e = 0.60$, $\Omega/\Omega_K = 2.64$, $r = 15 R_\odot$, $m = 2 M_\odot$. A similar pattern, except for a shift, is obtained with different values of e , Ω/Ω_K , m and r . For

any value of inclination, all points stretch out asymptotically to 3.9 for large values of the primary mass. This is due to the fact that for larger total mass of the system, greater is the distance to the periastron, and consequently, less deformation is expected. The light curve becomes flat.

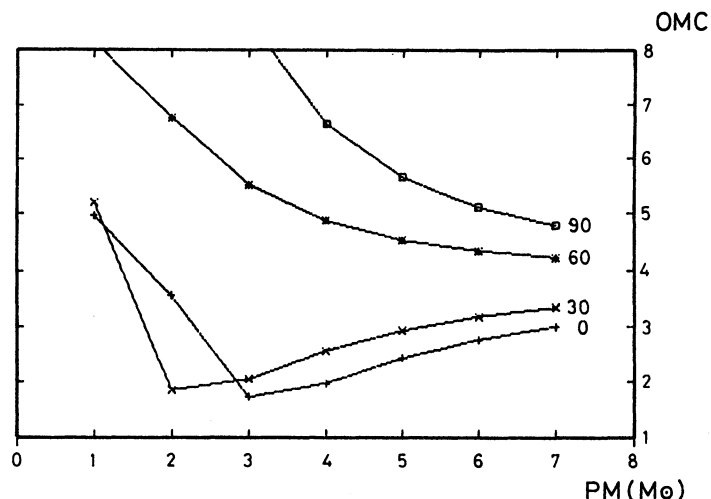


Fig. 4 Statistical parameter omc as a function of primary mass for different values of inclination. The values taken for the other parameters are $e = 0.60$, $\Omega/\Omega_K = 2.64$, $r = 15 R_\odot$ and $sm = 2 M_\odot$.

VI. RESULTS AND CONCLUSION

We have found values $omc \leq 2$ for eccentricities $0.45 \leq e \leq 0.70$ and for a synchronous rotation velocity. The values of the primary mass are less than $7 M_\odot$ for radius $10 \leq r \leq 20 R_\odot$ and for radius $r \geq 20 R_\odot$ the primary mass is $7 \leq pm \leq 13 M_\odot$.

If the rotational velocity of the primary star equals the periastron orbital angular velocity the solutions are quite similar, but we discard some of them because the major radius of the star at periastron is greater than the periastron distance.

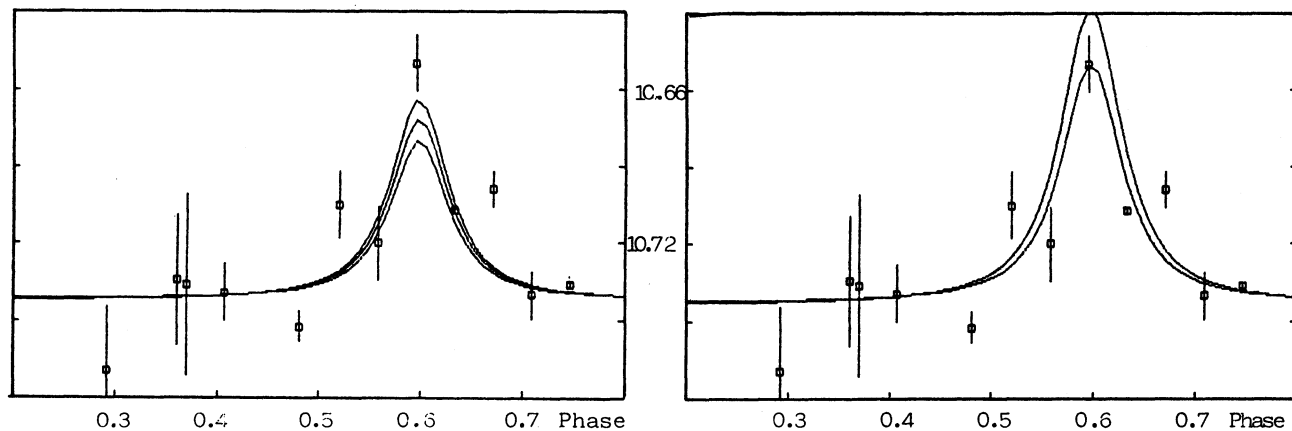


Fig. 5 Generated light curves. The parameters of the left figure are: $r = 21 R_\odot$, $pm = 8 M_\odot$, $sm = 2 M_\odot$, $i = 0$ and $e = 0.65$. The value of Ω/Ω_K is 1 (upper), 4 (middle) and 6.2 (below). The parameters of the right figure are: $r = 15 R_\odot$, $pm = 3 M_\odot$, $sm = 1.5 M_\odot$, $i = 0$ and $e = 0.65$. The value of Ω/Ω_K is 1 (upper) and 6.2 (below). The upper curve is the only one that has $omc > 2$.

In Figure 5 we represent some examples of the generated light curves. The similarity between the observed and the calculated light curves is acceptable, indicating that deformations of the primary by the secondary in an eccentric system can explain the observed optical variation. More observations are necessary in order to reduce the different possibilities of generated light curves similar to the observed values. The more acceptable physical solutions, according to the spectral type and luminosity class considered, correspond to larger masses.

REFERENCES

- Bartolini, C., Custodi, P., Dell'Atti, F., Guarnieri, A., and Piccioni, A. 1983, *Astr. and Ap.*, **118**, 365.
- Bignami, G.F., Caraveo, P.A., Lamb, R.C., Markert, T.H., and Paul, J.A. 1981, *Ap. J.*, **247**, L85
- Brown, J.C. and Boyle, C.B. 1984, *Astr. and Ap.*, **141**, 369.
- Carbon, D.F. and Gingerich, O. 1969, "Theory and Observation of Normal Stellar Atmospheres", *Proceedings of the Third Harvard-Smithsonian Conference on Stellar Atmospheres*, Ed. O. Gingerich, p.377.
- Clausen, J.V., Gyldenkerne, K., and Gronbech, B. 1977, *Astr. and Ap.*, **58**, 121.
- Coe, M.J., Bowring, S.R., Court, A.J., Hall, C.J., and Stephen, J.B. 1983, *M.N.R.A.S.*, **203**, 791.
- Hutchings, J.B. and Crampton, D. 1981, *Pub.A.S.P.*, **93**, 486.
- Kurucz, R.L. 1979, *Ap. J. Suppl. Ser.*, **40**, 1.
- Paredes, J.M. and Figueras, F. 1986, *Astr. and Ap.*, **154**, L30.
- Perotti, F., Della Ventura, A., Villa, G., Di Cocco, G., Butler, R.C., Dean, A.J., and Hayles, R.I. 1980, *Ap. J. (Letters)*, **239**, L49.
- Pollock, A.M., Bignami, G.F., Hermsen, W., Kanback, G., Lichti, G.G., Masnou, J.L., Swanenburg, B.N., and Wills, R.D. 1981, *Astr. and Ap.*, **94**, 116.
- Taylor, A.R. and Gregory, P.C. 1982, *Ap. J.*, **255**, 210.
- Taylor, A.R. and Gregory, P.C. 1984, *Ap. J.*, **283**, 273.
- Torra, J.T. and Nuñez, J. 1986, private communication
- Wood, D.B. 1971, *Astron. J.*, **76**, 8, p701
- Wood, D.B. 1973, *M.N.R.A.S.*, **164**, 53.

Josep-Maria Paredes: Departament de Física de la Terra i del Cosmos, Universidad de Barcelona, Diagonal 647, Barcelona 08028, España.